2018 IEEE 15th International Symposium on Biomedical Imaging (ISBI 2018)
April 4-7, 2018, Washington, D.C., USA

Radiomics Analysis of Baseline ^{18}F-FDG PET/CT Images for Improved Prognosis in Nasopharyngeal Carcinoma

Wenbing Lv[1], Qingyu Yuan[2], Quanshi Wang[2], Jianhua Ma[1,], Qianjin Feng[1], Wufan Chen[1], Arman Rahmim[3, 4], Lijun Lu[1,*],*

[1]School of Biomedical Engineering and Guangdong Provincial Key Laboratory of Medical Image Processing, Southern Medical University
[2]Nanfang PET Center, Nanfang Hospital, Southern Medical University
[3]Department of Radiology, Johns Hopkins University
[4]Department of Electrical and Computer Engineering, Johns Hopkins University

ABSTRACT

The purpose of this study is to investigate the prognostic performance of radiomics features on nasopharyngeal carcinoma (NPC) patients imaged with baseline ^{18}F-FDG PET/CT. 128 NPC patients were retrospectively enrolled with 3348 radiomics features and 13 clinical features. Kaplan-Meier analysis was used to estimate progression-free survival (PFS), and log-rank test was used to screen the significant features. Cox proportional hazards regression modal with forward stepwise feature selection was adopted to identify independent predictors of PFS. 24 radiomics features and 8 clinical features were found to be significantly associated with PFS in univariate analysis. Radiomics features HGZE_GLSZM_HLL_32 (p=0.0061, HR: 0.66, 95%CI: 0.49-0.89), as well as clinical features N-stage, M-stage, antibody VCA-IgA and platelet count (PLT) retained the independent prognostic significance for PFS in multivariate analysis. Overall, radiomics features can provide complementary prognostic information for NPC patients imaged with baseline ^{18}F-FDG PET/CT compared to clinical features.

Index Terms— Nasopharyngeal carcinoma, ^{18}F-FDG PET/CT, prognosis, radiomics, progression-free survival, clinical features

1. INTRODUCTION

Nasopharyngeal carcinoma (NPC) occurs with high frequency in southern China, with a peak annual incidence up to 30 per 100,000 [1]. ^{18}F-FDG PET has been increasingly used in the management of patient with NPC [2], and developments in radiotherapy and chemoradiotherapy have also improved the survival of NPC patients. However, local regional recurrence and distant metastasis remain the major causes of treatment failure [3], and early prediction of the outcome before treatment is thus crucial to perform individualized treatment.

Previous studies have investigated the TNM stage and image-based SUV parameters as well as total lesion glycolysis (TLG) as prognostic factors [4, 5]. Furthermore, clinical factors such as hemoglobin and platelet count also showed good prediction efficiency of survival [6]. In particular, plasma Epstein-Barr virus DNA load (EBV-DNA) has been identified as an independent prognostic marker for NPC [7]. Nevertheless, their reliability of outcome prediction still need to be further validated [3].

Given that malignant tumors are prone to be heterogeneous [8], quantitative description of intratumoral heterogeneity has been demonstrated to be useful for prognostication in various tumors [9-11]. Radiomics analysis, by extracting high throughput features from tumor image, can provide crucial information of tumor heterogeneity [12]. Law et al. identified diffusion-weighted imaging (DWI) parameters can predict local failure of patients with NPC [13]. Huang et al. first studied the heterogeneity factor, defined as the derivative of a volume threshold function of FDG uptake, to predict NPC patient outcome [9]. Chan et al. found that tumor heterogeneity characterized by texture features was superior to traditional PET parameters for predicting outcomes in primary NPC [14]. Zhang et al. developed a multiparametric MRI-based radiomics nomogram to improve the prognostic ability in advanced NPC [15]. Thus, radiomics features served as an image-based biomarker has showed its potential to diagnosis, prediction and prognosis.

This work was supported by the National Natural Science Foundation of China under grants 61628105, 81501541, the National key research and development program under grant 2016YFC0104003, the Natural Science Foundation of Guangdong Province under grants 2016A030313577, and the Program of Pearl River Young Talents of Science and Technology in Guangzhou under grant 201610010011.
*J. Ma, L. Lu (e-mail: jhma@smu.edu.cn, ljlubme@gmail.com)

However, to the best of our knowledge, prognostic analysis of NPC from ^{18}F-FDG PET images by using radiomics features has not been investigated. Thus, in the present study, we aim to use pretreatment radiomics features and clinical features as risk factors to evaluate progression-free survival of NPC patients imaged with ^{18}F-FDG PET.

2. MATERIALS AND METHODS

2.1. Patients and follow-up

This retrospective study was approved by IRB and informed consent was waived. From January 2012 to August 2016, 128 patients (103 men and 25 women; mean age, 47.7 years ± 13.2) with nasopharyngeal carcinoma confirmed by pathology were retrospectively enrolled in this study (Table 1). All patients received radiotherapy or chemoradiotherapy.

Progression free survival (PFS) was selected as the main endpoint, since its shorter follow up time than overall survival (OS) makes it possible to perform earlier intervention and further personalized treatment. PFS is defined as the time from the first day of treatment to the date of disease progression (local or regional recurrences or distant metastases), death from any cause, or the date of the last follow-up visit (censored). The mean follow-up time was 32 ± 9 months (range: 1-59 months). Progression was diagnosed by clinical symptoms, physical examination, flexible nasopharyngoscopy, biopsy, or radiation imaging methods (PET/CT, MRI et al.).

2.2. ^{18}F-FDG PET/CT protocol

All patients underwent a whole-body ^{18}F-FDG PET/CT scanning before treatment on a Siemens Biograph-128 mCT scanner at the Nangfang Hospital of Southern Medical University. Patients fasted for 6 hours before the radiotracer injection: 306-468 MBq (8.27-12.65 mCi) of ^{18}F-FDG (~150μCi/kg of body weight) was administered intravenously 60 minutes prior to PET/CT scanning. PET images were reconstructed using standard ordered-subset expectation maximization (OSEM) with 3 iterations and 21 subsets. CT scans (80mA, 120KVp) were used for attenuation correction. PET image with voxel size of $4.07 \times 4.07 \times 5$ mm^3 and matrix size of 200×200, was interpolated to the same resolution as CT voxel sizes of $0.98 \times 0.98 \times 3$ mm^3 and matrix size of 512×512 for registration/fusion and feature extraction purposes. The body weight SUVs were calculated for subsequent analysis.

2.3. Image preprocessing

In order to characterize intra-tumor heterogeneity more comprehensively, apart from original image, wavelet decompositions were also introduced to extract a number of radiomics features [16]. In this study, a discrete, one-level and undecimated 3D wavelet transform "Coiflet 1" was applied to each SUV image, by performing low-pass (L) or high-pass (H) filter along x-, y- or z- directions, resulting in 8 decompositions (LLL, LLH, LHL, LHH, HLL, HLH, HHL and HHH) of original image.

Two radiologists (Q. Yuan and Q. Wang with 3 and 10 years of experience in the interpreting of nasopharyngeal ^{18}F-FDG PET/CT images, respectively) were invited to delineate the 3D primary tumor on original image by using ITK-SNAP 3.4 software, and the intersection of two segmentation results was used for subsequent analysis.

Table 1 clinical characteristics of patients (N = 128).

Age, year, mean+_SD	47.7 ± 13.2
Sex, no.(%)	
Male	103 (80.5%)
Female	25 (19.5%)
T stage, no.(%)	
T1/T2	20 (15.6%)/20(15.6%)
T3/T4	54 (42.3%)/34 (26.5%)
N stage, no.(%)	
N0/N1	14 (10.9%)/33 (25.8%)
N2/N3	54 (42.2%)/27 (21.1%)
M stage, no.(%)	
M0/M1	101(78.9%)/27(21.1%)
AJCC stage, no.(%)	
I/II	4 (3.1%)/11 (8.6%)
III/IV	49 (38.3%)/64 (50%)

Before feature extraction, original image and the 8 decompositions (thus a total of 9 images) were discretized to 32, 64, 128 and 256 different values. Since the applied wavelet decomposition is undecimated, the size of each decomposition is equal to the original image. The original tumor delineation can be applied directly to the decompositions after wavelet transform. Thus, we obtained $9 \times 4=36$ discretized volumes of interest (VOIs) for each tumor.

2.4. Radiomics features

A total of 3348 radiomics features were investigated in this study, including 9 shape features extracted from the segmentation mask, 19 SUV features extracted on 9 VOIs ($19 \times 9=171$) and 88 texture features extracted on 9 VOIs under 4 types of discretization ($88 \times 9 \times 4=3168$). In addition to 57 conventional texture features, which are commonly appeared in various literatures, we also introduced 31 novel texture features to fully explore intra-tumor heterogeneity. The 57 conventional texture features consist of 26 gray level co-occurrence matrix-GLCM features, 13 gray level run length matrix-GLRLM features, 13 gray level size zone matrix-GLSZM features, and 5 neighborhood gray tone difference matrix-NGTDM features. The 31 novel texture features consist of 13 gray level gap length matrix-GLGLM features [17], 5 neighboring gray level dependence matrix-NGLDM features [18], 2 texture spectrum-TS features, 3 texture feature coding-TFC features,

Table 2 Univariate analysis of risk factor associated with PFS.

Clinical features	Cutoff	p	Texture features	Cutoff	p
Age (year)	53	0.003	LGLGE_GLGLM_Image_32	0.34	0.004
N stage	N0-N1 vs N2-N3	0.002	SumEntropy_GLCM_LLL_32	3.72	0.006
M stage	M0 vs M1	<0.001	GLV_GLRLM_LHL_32	0.03	0.009
VCA-IgA	- vs +	0.001	SAM_TFCM_LHL_32	0.01	0.010
EBV DNA (copies/mL)	7220	0.002	RLV_GLRLM_LHH_32	3.31×10^{-4}	0.001
LYM (10^9 g/L)	1.52	0.005	HGZE_GLSZM_HLL_32	288.25	0.006
HGB (g/L)	133	0.045	MaxSpe_TS_HLL_32	0.05	0.002
PLT (10^9 g/L)	213	0.032	LGLGE_GLGLM_Image_64	0.10	0.002
Shape features			SumEntropy_GLCM_LLL_64	4.42	0.006
Compactness1	1.46×10^{-4}	0.006	IMC2_GLCM_LLL_64	0.77	0.005
Compactness2	7.59×10^{-6}	0.006	GLV_GLSZM_HLL_64	2.00×10^{3}	0.003
Irregularity	52.43	0.006	LGLGE_GLGLM_Image_128	0.02	0.004
SUV features			SumEntropy_GLCM_LLL_128	5.12	0.005
Skewness_hist_LLL	0.68	0.003	Entropy_GLCM_HLL_128	8.13	0.004
Kurtosis_hist LLH	3.22	0.037	SumEntropy_GLCM_LLL_256	5.81	0.004
Entropy_hist_LLH	0.01	0.018	GLV_GLRLM_LLL_256	0.05	0.002
AUC_CSH_LHH	0.45	0.024			
Kurtosis_hist_LHH	6.78	0.017			

LGLGE: long gap low gray level emphasis; GLV: gray level variance; SAM: the second angular moment; RLV: run length variance; HGZE: high gray level zone emphasis; IMC2: information measure of correlation 2;

and 8 texture feature coding method-TFCM features [19].

2.5. Clinical features

13 clinical features were obtained from the medical records. Age, sex, initial T, N, M staging category, AJCC stage, pretreatment plasma EBV DNA, immunoglobulin A antibodies against EBV viral capsid antigen (VCA-IgA), lymphocyte count (LYM), neutrophil count (NEUT), hemoglobin (HGB), platelet count (PLT), and lactate dehydrogenase level (LDH) were evaluated in this study.

2.6. Statistical analysis

Kaplan-Meier method was used to estimate progression free survival (PFS), the optimal cutoff point of each individual feature was selected when the lowest p value was observed, and two group patients with nearly equal number of members, and log-rank test was used to screen the significant features. Multivariate Cox proportional hazards regression modal with forward stepwise feature selection was adopted to identify the independent predictors of PFS. All statistical analyses were conducted by using MATLAB R2012a (The MathWorks Inc.), $p<0.05$ was considered statistically significant.

3. RESULTS

3.1. Patients characteristics

At the end of follow-up, 60 patients had come to progression (28 recurrence, 17 metastasis and 15 died). The MATV of 128 patients was 50.86 ± 86.43, range: 0.89-755.89 mm^3, the SUVmax was 15.43 ± 7.77, range: 1.70-41.41, and the SUVmean was 7.95 ± 3.75, range: 1.07-21.43.

3.2. Univariate analysis of prognostic factors

In univariate analysis, 8 clinical features, 3 shape features, 5 SUV features and 16 texture features were found to be significantly associated with survival rate (Table 2).

3.3. Multivariate analysis

Features that showed significant correlation with PFS rate in univariate analysis were entered into multivariate Cox regression modal. After adjustment for potential confounders, only four clinical features and one radiomics features retained the independent prognostic significance for PFS (Table 3). M stage ($p<0.0001$, HR: 4.10), VCA-IgA ($p=0.0071$, HR: 2.33), N stage ($p=0.002$, HR: 1.85), PLT ($p=0.0117$, HR: 0.69), HGZE_GLSZM_HLL_32 ($p=0.0061$, HR: 0.66). Figure 2 showed the Kaplan-Meier curves of PFS rates with these five features.

4. DISCUSSION

This study demonstrated that 24 radiomics features and 8 clinical features on NPC patients imaged with ^{18}F-FDG PET scanner were significantly associated with PFS in univariate analysis. While after multivariate analysis, only 1 radiomics features and 4 clinical features retained the independent prognostic significance for PFS.

In univariate analysis, those useful texture features were extracted at different discretization bins (range from 32 to 256), probably meaning that specific discretization bins are most suitable for specific features, and it also confirmed that the robustness of features can be affected by discretization [20]. Besides, those features also extracted from different wavelet decomposition images, indicating that some valuable information could hardly be excavated in original

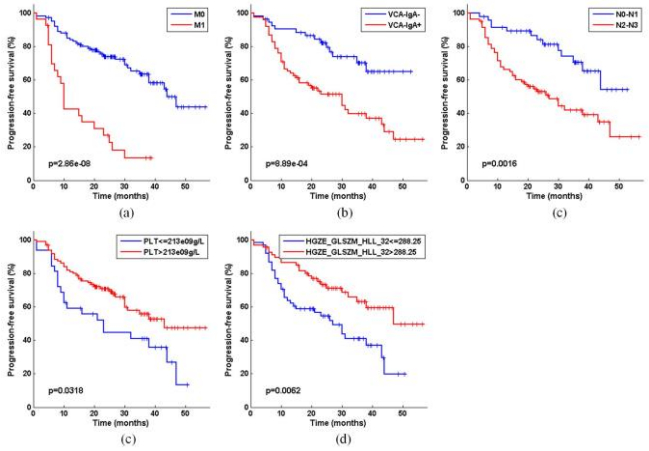

Figure 2. Kaplan-Meier curves of PFS rates with (a) M stage, (b) VCA-IgA, (c) N stage, (d) PLT and (e) HGZE_GLSZM_HLL_32. P-value was calculated by log-rank test.

Table 3 Multivariable analysis of risk factors associated with PFS in patients with nasopharyngeal carcinoma.

Risk factor	HR (95% CI)	p
M	4.10 (2.29-7.37)	<0.0001
VCA-IgA	2.33 (1.24-4.38)	0.0071
N	1.85 (1.33-2.59)	0.0002
PLT	0.69 (0.52-0.93)	0.0117
HGZE_GLSZM_HLL_32	0.66 (0.49-0.89)	0.0061

HGZE: high gray level zone emphasis.

image; filtered image may highlight the inconspicuous prognosis information.

In multivariate analysis, higher HGZE_GLSZM_HLL_32 or PLT independently predicted a lower PFS, in contrast to N, M classification and VCA-IgA whose higher value predicted a higher PFS. Thus, image-based quantitative features provided complementary information compared with clinical features.

One limitation of this study is that independent validation set is needed. Along this line, whether the combination of radiomics features and clinical features can improve prognostic stratification of PFS needs to be further investigated and validated in the future.

5. CONCLUSION

Radiomics features of pretreatment ^{18}F-FDG PET images that quantitatively characterize the intra-tumor heterogeneity can provide complementary prognostic information for NPC patients compared with clinical features. Adjustment of treatment options and individualized treatment thus can be potentially performed.

6. REFERENCES

[1] W.I. Wei, and J.S. Sham, "Nasopharyngeal carcinoma", *Lancet*, vol. 365, no. 9476, pp. 2041-2054, 2005.

[2] H. Zhou et al., "^{18}F-FDG PET/CT for the Diagnosis of Residual or Recurrent Nasopharyngeal Carcinoma After Radiotherapy: A Metaanalysis", *J. Nucl. Med.*, vol. 57, no. 3, pp. 342-347, 2016.

[3] A.W. Lee, B.B. Ma, W.T. Ng, and A.T. Chan, "Management of Nasopharyngeal Carcinoma: Current Practice and Future Perspective", *J. Clin. Oncol*., vol. 33, no. 29, pp. 3356-3364, 2015.

[4] S.C. Chan et al., "Clinical utility of 18F-FDG PET parameters in patients with advanced nasopharyngeal carcinoma: predictive role for different survival endpoints and impact on prognostic stratification", *Nucl. Med. Commun*., vol. 32, no. 11, pp. 989-996, 2011.

[5] K.P. Chang et al., "Prognostic significance of 18F-FDG PET parameters and plasma Epstein-Barr virus DNA load in patients with nasopharyngeal carcinoma", *J. Nucl. Med*., vol. 53, no. 1, pp. 21-28, 2012.

[6] H. Chang et al., "Haemoglobin, neutrophil to lymphocyte ratio and platelet count improve prognosis prediction of the TNM staging system in nasopharyngeal carcinoma: development and validation in 3,237 patients from a single institution", *Clin Oncol (R Coll Radiol)*, vol. 25, no. 11, pp. 639-646, 2013.

[7] W.Y. Wang et al., "Long-term survival analysis of nasopharyngeal carcinoma by plasma Epstein-Barr virus DNA levels", *Cancer-Am. Cancer Soc*., vol. 119, no. 5, pp. 963-970, 2013.

[8] J.P. O'Connor et al., "Imaging intratumor heterogeneity: role in therapy response, resistance, and clinical outcome", *Clin. Cancer Res.*, vol. 21, no. 2, pp. 249-257, 2015.

[9] B. Huang, T. Chan, D.L. Kwong, W.K. Chan, and P.L. Khong, "Nasopharyngeal carcinoma: investigation of intratumoral heterogeneity with FDG PET/CT", *AJR Am J Roentgenol*, vol. 199, no. 1, pp. 169-174, 2012.

[10] N.M. Cheng et al., "Textural features of pretreatment ^{18}F-FDG PET/CT images: prognostic significance in patients with advanced T-stage oropharyngeal squamous cell carcinoma", *J. Nucl. Med.,* vol. 54, no. 10, pp. 1703-1709, 2013.

[11] K.G. Foley et al., "Development and validation of a prognostic model incorporating texture analysis derived from standardised segmentation of PET in patients with oesophageal cancer", *Eur. Radiol.*, 2017.

[12] V. Parekh, and M.A. Jacobs, "Radiomics: a new application from established techniques", *Expert Rev Precis Med Drug Dev*, vol. 1, no. 2, pp. 207-226, 2016.

[13] B.K. Law et al., "Diffusion-Weighted Imaging of Nasopharyngeal Carcinoma: Can Pretreatment DWI Predict Local Failure Based on Long-Term Outcome?", AJNR Am J Neuroradiol, vol. 37, no. 9, pp. 1706-1712, 2016.

[14] S.C. Chan et al., "Tumor heterogeneity measured on F-18 fluorodeoxyglucose positron emission tomography/computed tomography combined with plasma Epstein-Barr Virus load predicts prognosis in patients with primary nasopharyngeal carcinoma", Laryngoscope, vol. 127, no. 1, pp. E22-E28, 2017.

[15] B. Zhang et al., "Radiomics Features of Multiparametric MRI as Novel Prognostic Factors in Advanced Nasopharyngeal Carcinoma", *Clin. Cancer Res.*, vol. 23, no. 15, pp. 4259-4269, 2017.

[16] H.J. Aerts et al., "Decoding tumour phenotype by noninvasive imaging using a quantitative radiomics approach", *Nat. Commun.*, vol. 5, pp. 4006, 2014.

[17] X. Wang, A. Fritz, and F. Bent, "Texture Features from Gray level Gap Length Matrix", *MVA'94 IAPR workshop on machine vision applications*, 1994.

[18] C. Sun, and W.G. Wee, "Neighboring Gray Level Dependence Matrix for Texture Classification", *computer vision, graphics, and image processing*, vol. 23, pp. 341-352, 1982.

[19] M.H. Horng, Y.N. Sun, and X.Z. Lin, "Texture feature coding method for classification of liver sonography", *Comput Med Imaging Graph*, vol. 26, no. 1, pp. 33-42, 2002.

[20] L. Lu et al., "Robustness of Radiomic Features in [C-11]Choline and [F-18]FDG PET/CT Imaging of Nasopharyngeal Carcinoma: Impact of Segmentation and Discretization", *Mol. Imaging Biol.*, vol. 18, no. 6, pp. 935-945, 2016.